International Research Journal of Engineering and Technology (IRJET) e-ISSN: 2395-0056
Volume: 11 Issue: 03 | Mar 2024 www.irjet.net p-ISSN: 2395-0072

Liquid Cooled Thermal Management System for Lithium-Ion Batteries: A recent review

Kirti Mangliya[1], Vivek Trivedi[2]

[1]ME Scholar, Dept. of Mechanical Engineering, L.D. College of Engineering, Gujarat, India.
[2]Assistant Professor, Dept. of Automobile Engineering, L.D. College of Engineering, Gujarat, India.

Abstract - *Traditional fuels and internal combustion engines are the largest sources of carbon dioxide emissions and cause environmental pollution. Electric vehicles (EV) are considered a green energy solution for a pollution-free future. The importance of the environment has grown significantly in recent years, and companies operating in several technological sectors are moving towards environmentally friendly solutions. One of the most discussed topics in the automotive industry is lithium-ion batteries for electric vehicles and their battery thermal management systems (BTMS). Electric cars use Li-ion batteries for energy storage and have many challenges, such as low efficiency at low and high temperatures, high temperature electrode life, and safety issues related to the thermal drainage of Li-ion batteries, which directly affect performance, vehicle reliability, price and safety. Overheating caused by the movement of electrons during chemical reactions during the process of charging and discharging at high temperatures can cause batteries to die. That's why an efficient battery thermal management system (BTMS) is one of the most important technologies for the long-term success of electric vehicles. As the use of lithium-ion batteries increases, higher demands are placed on battery thermal management systems. Compared with other cooling methods, liquid cooling is an effective cooling method that can control the maximum temperature and maximum temperature difference of the battery within a reasonable range. This article reviews the latest research on thermal management systems for liquid-cooled batteries from the perspective of indirect liquid cooling.*

Key Words: **electric vehicle; battery thermal management system; liquid cooling; indirect liquid cooling; CFD simulations; heat transfer**

1. INTRODUCTION

As the energy crisis and environmental pollution become prominent, the vigorous development of clean energy, the improvement of the environment and the promotion of green and low CO_2 construction have become an important task. Conventional fuel vehicles run mainly on non-renewable fossil energy, which not only consumes more fossil energy, but also produces emissions that contribute to the greenhouse effect. In this context, electric vehicles have attracted much attention due to their advantages such as low pollution and high efficiency [1]. A central task in the development of electric vehicles is to find a suitable energy storage system that allows battery vehicles to drive for a long time and accelerate quickly. Current lithium-ion batteries (LIB's) have been widely used in electric vehicles and have high specific energy, high specific capacity, low self-discharge rate, high voltage, relatively long service life and good recyclability is considered the most suitable energy storage for electric vehicles [2]. However, the operating and uniform storage temperature affects the performance of Li-ion batteries. In general, the optimal operating temperature range of Li-ion batteries is 15-40°C, and the maximum temperature difference of the batteries should be regulated within 5°C [3]. The maximum temperature rise is the maximum difference between the battery temperature and the ambient temperature. The maximum temperature difference is the maximum difference value stored in the battery. High temperatures increase the reaction rate resulting in higher power and output but at the same time cause even higher temperatures and increased heat load [4]. If the heat is not dissipated at least as fast as it is generated in the batteries, temperatures can rise uncontrollably, leading to degradation of materials and components or even thermal runaway of the batteries. Thermal runaway is an event that leads to a sudden increase in temperature, gas formation and even battery explosion, which endangers the safety of the vehicle and its occupants [5]. Therefore, a reasonable and efficient battery thermal management system (BTMS) is necessary for the safe operation of the battery module and good charging and discharging performance. There are two main sources of heat production in a battery cell which are electrochemical action and joule heating caused by the movement of electrons in the battery cells [6]. The temperature of 15°C to 40°C provides ideal working conditions for lithium-ion batteries, and if the temperature rises above 50°C, it becomes harmful to the life of the batteries. Premature wear of even one cell can significantly reduce the performance and efficiency of the entire battery [7]. The main purpose of BTMS is to regulate the temperature of the battery cells and thus extend the life of the battery. Currently popular BTMSs can be divided into air cooling, liquid cooling, phase change material (PCM), heat pipes and composite cooling.

2. Heat Generation Mechanism and Temperature Effects

2.1. Heat Generation Mechanism

Lithium-ion batteries consist of four parts: anode (negative electrode), cathode (positive electrode), electrolyte and separator. During battery charging and discharging, as shown in Figure 1, Lib's discharge back and forth between the positive and negative electrodes through the electrolyte and separator, hence the name "rocking chair battery". During charging, lithium ions receive energy from the outside, move to anode, and sink to the anode, forming an ion space rich in lithium ions on the anode. During discharge, lithium ions transport energy from the negative electrode, while electrons move back and forth through the external circuit, generating current during charging and discharging.

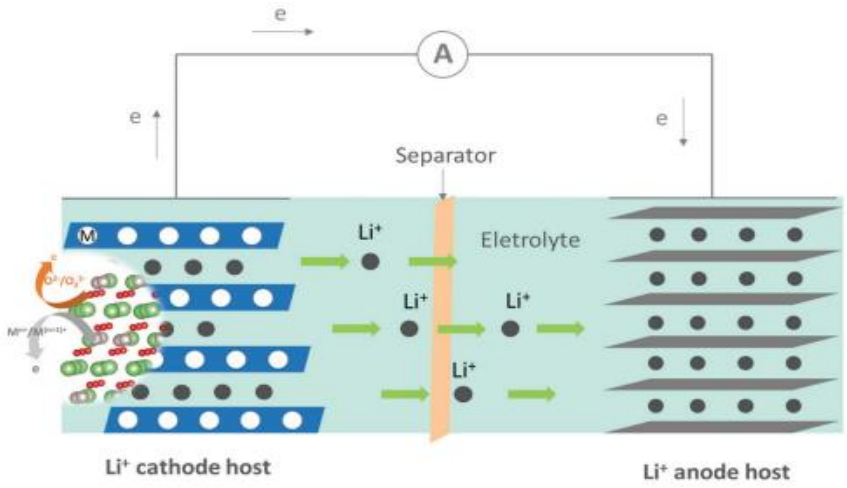

Figure 1. Diagram of the working principle of a lithium-ion battery (LIB) [8].

During the normal charging and discharging of a battery, a large number of chemical reactions take place inside the battery, and these complex chemical reactions usually involve the generation of heat. If the heat cannot be dissipated in time, the temperature of the battery will rise rapidly with the continuous generation and accumulation of heat, causing a series of abnormal side reactions that will cause the performance of the battery to deteriorate and even trigger thermal runaway. Therefore, it is necessary to investigate the heat generation mechanism of LIB. Broadly speaking, LIB heat production can be divided into two parts: renewable heat and irreversible heat. Reversible heat is the heat released when lithium ions are decalcified between the positive and negative electrodes. This is due to the reversible entropy change caused by the electrochemical reaction inside the battery, also called heat of reaction or heat of entropy. Irreversible heat includes polarization heat and ohmic heat [9]. Polarization heat results from lithium ions overcoming resistance during internal motion, while ohmic heat or Joule heat is associated with resistance within the battery.

One of the most commonly used battery heat generation equations proposed by Bernardi [10] is used to predict the heat generation rate of an individual battery. The expression is

$$Q = I(E - U) - IT\frac{DE}{DT} \tag{1}$$

where Q, I, E, U and T are expressed as heat generating power, operating current, cut-off voltage, operating voltage and operating temperature. The first term I $(E - U)$ on the right represents irreversible heat. The second term ***-IT(DE/DT)*** represents reversible heat, which is negative during charging and positive during discharging, while the thermal coefficient of entropy ***(DE/DT)*** is related to density, state of charge (SOC), and battery temperature. The heat generation model has been widely used because of its convenient operation and reasonable accuracy, but it does not consider the existence of phase change heat and heat of mixing. In case of irreversible heat ***(E – U)*** can be replaced by ***IR; R*** represents the internal resistance of the battery and the formula can be simplified as follows:

$$Q = I^2R - IT\frac{DE}{DT} \tag{2}$$

Compared to the non-recoverable heat, the recoverable heat can be negligible in practical hybrid electric vehicles and pure electric car applications. Therefore, the formula can also be expressed in the form [11]:

$$Q = I^2R - IT\frac{\Delta S}{F} \quad (3)$$

where ΔS represents the entropy change, which is negative during charging and positive during discharging. F is Faraday's constant.

2.2. Temperature Effects

Battery performance and state of health (SOH) are strictly dependent on the temperature of the operating environment. A large amount of heat is generated inside the package, especially during the rapid loading and unloading process due to several chemical reactions and electrochemical transport phenomena that increase the temperature of the battery.

The heat generated is greatest because hundreds of cells are connected in series or parallel, and the irregularity and thermal conditions of the battery cause a temperature difference between them. The exothermic existence of all these reactions indicates that temperature affects battery performance and heat remains inside the battery if it is not sufficiently dissipated. It has been found that the voltage, electricity, efficiency and life cycle of a cell are profoundly affected by its operating temperature. Temperature uniformity has a significant effect on the condition of the battery in the long term. Lithium-ion batteries have two important issues: First, the operating temperature exceeds the appropriate temperature limit. Second, low temperature uniformity reduces battery life.

2.2.1. Low Temperature Operating

The LIB below the optimal temperature range can degrade battery performance, limiting its use in cold environments. Low ambient temperature causes many problems, such as high resistance to accept charge. battery life and performance. The charger cannot charge the battery quickly when the battery is operating below 5°C. When the battery temperature is below 0°C, it loses charge, power, acceleration and range. It found that when the battery is used for a long time at a lower ambient temperature, the battery anode corrodes the lithium brick, reducing the safety of the battery. Smart et al. [12] showed that charging a battery at maximum capacity is difficult because lithium deposition can occur at high charge levels at room temperature.

2.2.2. High Temperature Operating

At high temperatures, as the temperature continues to rise, LIBs undergo a series of reactions that affect their performance. The solid electrolyte interface (SEI) film is first degraded at 90 °C or even lower. During the first charge-discharge cycle of a LIB, a passivation layer called SEI is created on the surface of the negative electrode. It can successfully prevent the organic solvent in the electrolyte from damaging the electrode material, thus improving the battery performance. Second, lithium reacts with the electrolyte. Then after 135°C the separator melts which causes a short circuit between the two electrodes [13]. When the temperature rises to 200°C, it triggers a series of complex reactions. As lithium ions and electrolytes are consumed in large quantities, the capacity and performance of the battery will decrease dramatically. Zhao et al. [14] highlighted that every 1°C increase in temperature between 30°C and 40°C shortens battery life by two months. Ramadass et al. [15] compared charge-discharge cycles at room temperature, 45°C, 50°C, and 55°C. The results showed a battery capacity loss of 30% after 800 cycles at a room temperature and a capacity loss of up to 70% after 490 cycles at 55°C. As the temperature and number of cycles increased, this reduced capacity and higher impedance reduced battery performance.

3. Battery Thermal Management Systems

The basic types of BTMS are listed below;

1. Air cooling
2. Direct refrigerant cooling
3. Phase change material cooling
4. Heat pipe cooling
5. Thermoelectric cooling
6. Liquid cooling

3.1. Air cooling

Air systems use air as a heat carrier. The incoming air can be either directly from the atmosphere or from the cabin, and this air can also be cleaned after the heater or evaporator of the air conditioner. The first is called a passive air system and the second is called an active air system. Active systems can provide additional cooling or heating capacity. A passive system can provide hundreds of watts of cooling or heating power, and the active power of the system is limited to 1 kW [16]. Since in both cases the air is supplied by a fan, they are also called forced systems.

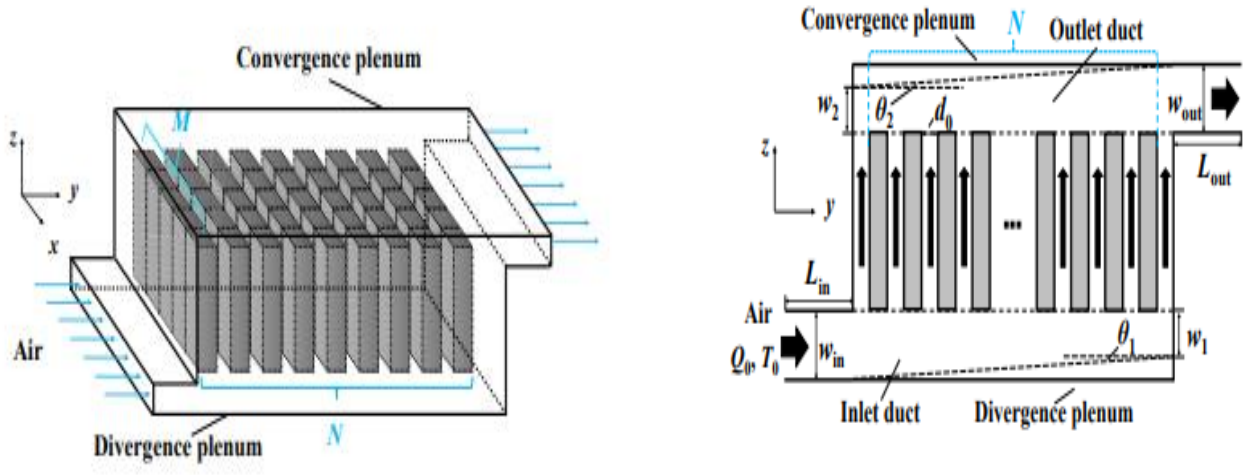

Figure 2. Air cooling system [16].

3.2. Direct Refrigerant cooling

Like active fluid systems, the Direct Refrigerant System (DRS) consists of an air conditioner circuit, but the direct refrigerant system uses the refrigerant directly as a heat transfer fluid that circulates through the coil [6].

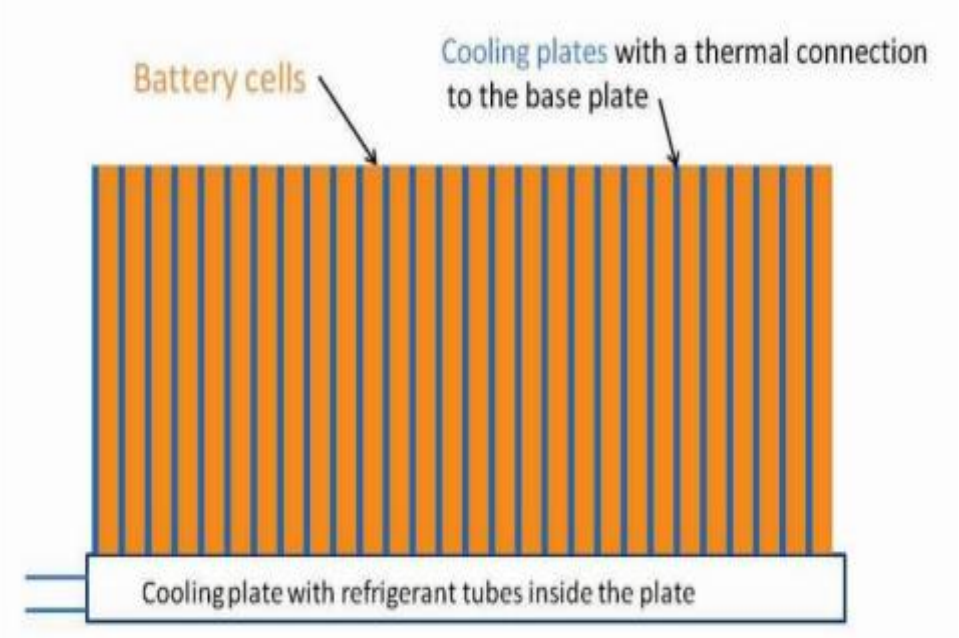

Figure 3. Direct Refrigerant Liquid Cooling [6].

3.3. Phase Change Material

The phase change material absorbs heat during the melting process and stores it as latent heat until it reaches a maximum value. The temperature is held at the melting temperature for a while and then the temperature rise is delayed. Hence PCM is used as a driver and buffer in BTMS. In addition, the PCM is always connected to another BTMS system, such as a liquid or air-cooling system, to monitor the internal temperature of the battery [17].

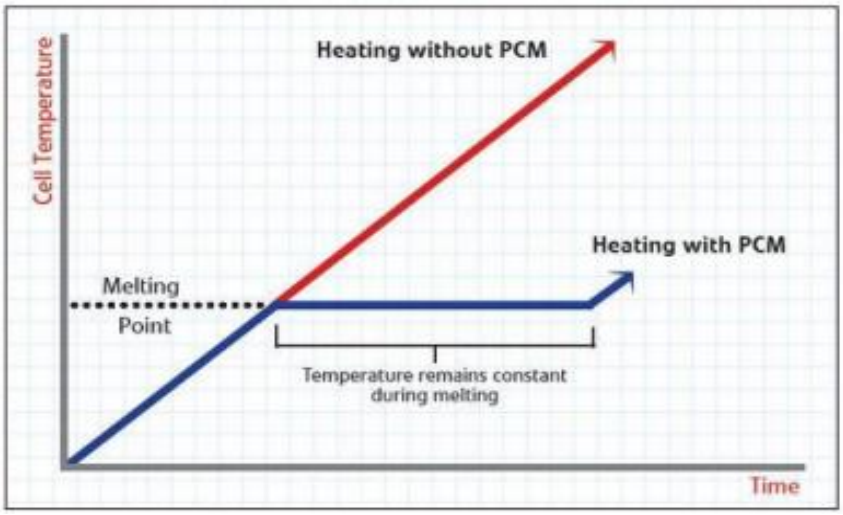

Figure 4. The working mechanism of PCM on battery cells [17].

3.4. Heat pipe cooling

It is a passive cooling system, which is basically a closed tube filled with refrigerant, which absorbs heat by evaporating the refrigerant on the hot side, and it removes the heat to the environment by condensing the refrigerant back into a liquid, forming on the cold side. and then flows back a partial vacuum which is maintained in the heat pipe body, and a capillary structure is used inside the heat pipes to increase the heat transfer rate of the heat pipes, which raises the surface temperature. The heat pipe can use water or any coolant like the coolant and this cycle repeats itself over and over. The battery acts as a heat source and is located under the heat pipe (evaporation side), and the cooling fins act as heat sinks in the heat pipe (condensation side). According to tests, a 30% reduction in thermal resistance was observed in a heat pipe cooling system with natural convection compared to without a heat pipe. In case of convection with low air speed, the thermal resistance decreases by 20%. The main problem with this cooling is the security of the system, which can be a concern in an emergency; a battery cell coolant leak can cause a short circuit that can cause vehicle failure and death. Capillary tubes also require a minimum diameter to maintain adequate pressure drop and prevent clogging [18].

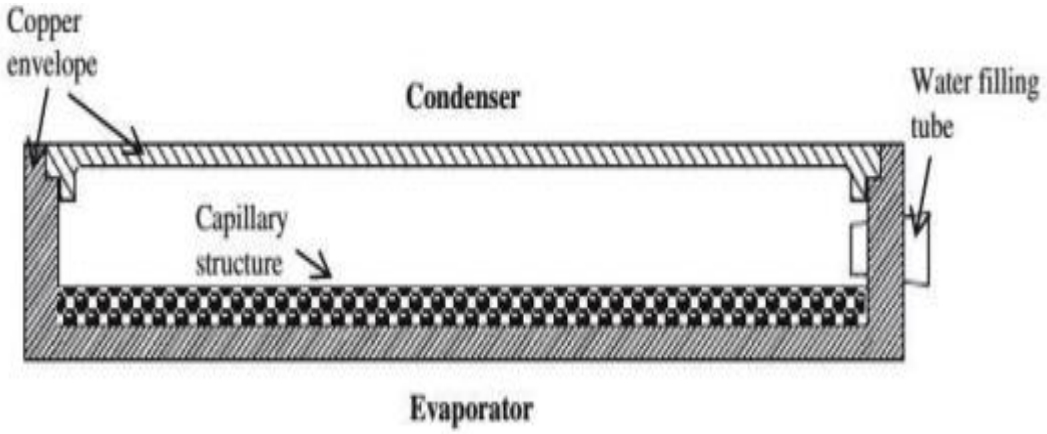

Figure 5. Structure of the heat pipe [18].

3.5. Thermoelectric cooling

There are two possible upgrades to improve the cooling/heating of passive air systems. One is through thermoelectric modules. A thermoelectric cooling system converts an electrical voltage into a temperature difference and vice versa. This section discusses the conversion of electrical voltage to temperature. It removes heat through the components by discharging electricity directly. The fans are equipped with forced convection to improve heat transfer. Mixing the passive air system with the thermoelectric system and the connected system cools the battery temperature even lower than the incoming air temperature, and the power is limited to less than one kW [6]. It can be used to switch between cooling and heating functions and only the polarity of the electrodes needs to be changed.

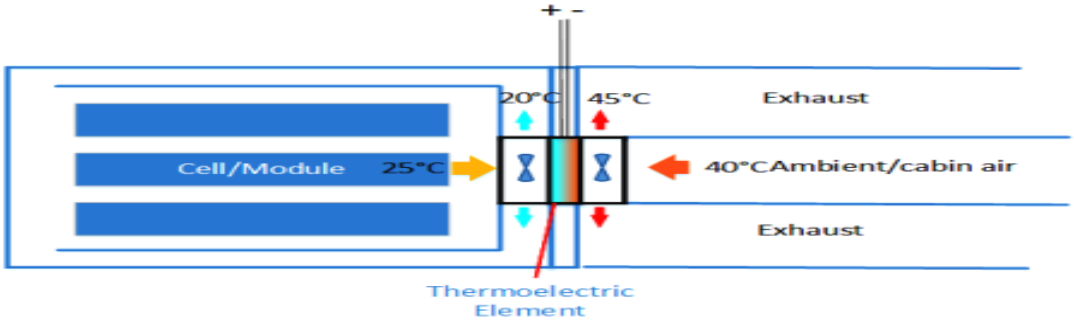

Figure 6. Thermoelectric cooling/heating system [6].

3.6. Liquid cooling

It is a cooling system that uses water as a coolant to cool the battery. Liquid cooling is the most commonly used cooling system due to its convenient design and good cooling capacity. Liquid cooling can be divided into indirect and direct cooling (also known as immersion cooling) depending on whether the cooling liquid is in contact with the battery, as shown in Figure 7. Indirect liquid cooling usually involves placing heat sinks, separate pipes or enclosures on the surface of the cell [19]. This cooling technology transfers the heat produced by the battery to the outside with the flowing coolant, avoiding direct contact between the coolant and the battery. With direct liquid cooling, the coolant is in direct contact with the battery, which requires the use of a non-conductive coolant. Direct liquid cooling greatly improves the contact surface between the battery and the coolant, resulting in very high heat transfer rates. Direct liquid cooling can be divided into single-phase and two-phase according to whether there is a phase change in the cooling liquid. Compared with indirect liquid cooling, direct liquid cooling has a better cooling effect and can improve the uniformity of temperature distribution [20]. Liquid cooling lends itself easily to prismatic cells due to their regular shape, which allows for compact BTMS placement, while cylindrical cells require special structures to integrate cooling channels, increasing system complexity and weight. For prism and pouch batteries, the most common solution is to apply cooling plates. General studies analyse temperature and velocity distribution in cooling plates. In this section, the main research progress of indirect liquid cooling is introduced.

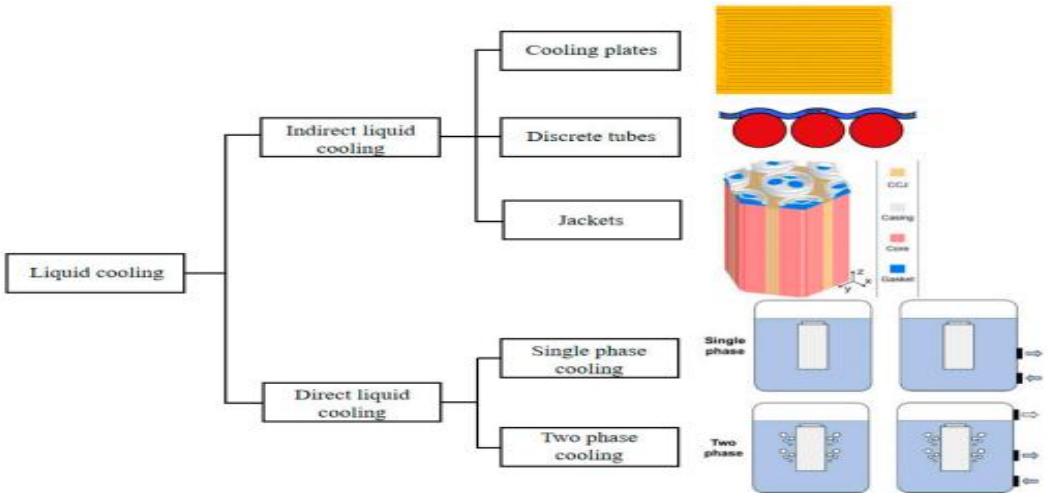

Figure 7. Classification of liquid cooling [3].

3.6.1. Direct Liquid Cooling

In the direct liquid cooling system, the refrigerant and the battery are in direct contact, which increases the heat transfer process and simplifies the system structure, and reduces the contact thermal resistance. The refrigerant of the liquid direct cooling system must be well insulated, non-flammable and environmentally friendly. Commonly used fluids are silicone oil, transformer oil, fluoroether, etc. Compared with indirect liquid cooling, it can save space and cost and reduce overall weight, but in terms of energy consumption, direct liquid cooling systems require more energy because the coolant has high viscosity [13]. Several researchers have found that direct liquid cooling systems for BTMS may not be suitable for use due to their higher viscosity, which consumes more energy than indirect liquid cooling [3].

3.6.2. Indirect Liquid Cooling

In the case of indirect liquid cooling, different forms of batteries are suitable for different cooling devices. Cylindrical batteries usually use separate tubes or casing to increase the contact area between the surface and the coolant. For prismatic batteries or lidded bags, flat cold plates are usually the best choice. The air gap between the heat sink or tube and the battery contributes to thermal insulation and reduces heat transfer efficiency because the coolant and battery are not in direct contact with each other. To eliminate air gaps, high-precision cold metal plate and grease or epoxy binder with high thermal conductivity are required to reduce thermal contact resistance [21]. In order to improve the removal of heat from the battery, researchers have done a lot of research on indirect liquid cooling. Selection of coolants, design of flow channels and optimization of system structures have received much attention and these studies are discussed in this section.

3.6.2.1. Coolant

Coolant viscosity, density, thermal conductivity, specific heat capacity, and flow rate are important variables that determine the cooling capacity and heat transfer efficiency of a liquid cooled BTMS. In order for the pumping power not to increase and the cooling capacity of the system to improve, a coolant with high thermal conductivity and low viscosity is needed. Because water is the simplest fluid in life, it has been widely used in indirect liquid cooling systems. It has been found that using water as a coolant can ensure battery temperature uniformity and improve BTMS cooling. In addition, water has a higher thermal conductivity and specific heat capacity than air and a lower viscosity than oil, which ensures heat transfer capacity and helps reduce additional energy consumption. To lower the freezing point of water so that BTMS can be used at lower temperatures (sub-zero), a water/glycol mixture is typically used as the coolant. The addition of glycol to the water can greatly extend the use of the BTMS and reduce the risk of battery damage due to the increased volume due to condensation of the water. To eliminate short-circuit problems caused by contact with the battery after liquid leakage, water or water/glycol-based BTMS should strictly avoid direct contact between the coolant and the battery [22].

Wang et al [23] investigated the performance of hollow cold plates for pouch lithium-ion batteries using 50% aqueous ethylene glycol as the coolant. The effect of mass flow of coolant on the maximum temperature of the battery was investigated. The maximum cell temperature gradually decreases as the mass flow rate (qm) increases. When qm is 0.01 kg/s, the highest peak temperature of the cell is 38.3 °C at 720 s, and it decreases by 2.6 °C when qm is 0.005 kg/s, with a reduction rate of 6.36%. When qm is 0.015 kg/s, the highest maximum cell temperature appears at 630 s and decreases by 1.6 °C when qm is 0.01 kg/s, with a decrease rate of 4.18%. When qm is 0.02 kg/s, the maximum highest temperature is 35.4 °C at 570 s and it decreases by 1.3 °C when qm is 0.015 kg/s and the decrease rate is 2.99%. When qm is 0.025 kg/s, the highest maximum temperature appears at 540 s, which is 0.9 °C lower, and the reduction rate is 2.54%. Thus, it can be seen that when qm is greater than 0.01 kg/s, the maximum temperature first increases and then decreases with discharge time, and both are below 40 °C. Aldosry et al. [24] used two types of fluids in their study, namely G13 ethylene glycol and distilled water in five stages, 10% ethylene glycol, 100% distilled water, 75% ethylene glycol + 25% distilled water, 50% ethylene glycol + 50% distilled water and 25 % ethylene glycol + 75 % distilled water. Three different flow rates of 0.3, 0.5 and 0.7 grams per minute (GPM) were used to maximize fluid and heat transfer productivity through the gate valve. The cold plate consists of an inclined fin, which is able to increase the rate of heat transfer from the heater to the liquid cold plate. The GPM 0.7 achieved the lowest battery surface temperature at three different flow levels. The cold plate can keep the surface temperature around the batteries slightly below the permitted operating temperature of 50°C. Pan et al. [25] investigated the effects of the number of channels, cold plate panel thickness, coolant mass flow rate, and cooling tube thickness on the cooling efficiency of a battery system. The heat dissipation performance of the battery was found to be slightly impacted by the thickness of cooling plate or cooling tube during the orthogonal test, but significantly influenced by how many cooling channels and cooling mass flow rate. A simpler method also revealed that these variables had little

impact on this factor. By increasing the mass flow rate of coolant, it is found that it's an effective way to increase heat dissipation from the battery.

In addition to investigating coolants with different thermal conductivities to improve the cooling performance of BTMS, some researchers also investigated coolant inlet temperature. Panchal et al. [26] designed a microchannel cold plate for cooling the prismatic battery and investigated the effect of water cooling at three operating temperatures of the, 5°C, 15°C and 25°C. Coolant temperature was found to affect the cooling of the cold plate. Malik et al. [27] investigated the performance of a battery at different cooling temperatures (10°C, 20°C, 30°C and 40°C) based on a cold plate. Test results showed that battery performance improved as the coolant temperature increased. They found that when the temperature of the coolant is 30°C, the maximum and average temperature of the battery can be controlled between 25°C and 40 °C at either a low discharge rate or a high discharge rate.

Water-based coolants have a lower viscosity and a higher heat transfer coefficient than most petroleum coolants. To further improve thermal conductivity, metal particles or metal oxides such as Al, Cu, Ag, Ni, alumina, titanium dioxide, silicon dioxide, etc. can be added to common liquid refrigerants. Coolants with added liquid metals and nanoparticles may be considered a better alternative to indirect liquid cooled BTMS water or water/ethylene glycol solution cooled coolants. If metal particles are added to traditional fluids, they become nanofluids. When added, the thermal conductivity of coolant increases significantly. As a result, the thermal conductivity of metal is much higher than that of conventional heat transfer fluids. Zakaria et al. [28] investigated the effect of Al_2O_3 (aluminium oxide) nanoparticles at different volume concentrations (0.1, 0.3 and 0.5%) on thermal conductivity in a water/glycol mixture. The results showed that the thermal conductivity increased when the concentration of nanoparticles was in the water/glycol mixture. In the water/glycol mixture with a 1:1 volume ratio of the nanoparticle volume concentrations was 0.1%, 0.3%, and 0.5%, and the thermal conductivity increased by 2%,4.2% and 7.5%. respectively. Maheshwari et al. [29] investigated the effect of concentration, size, and shape of TiO_2 (titanium dioxide) nanoparticles on the thermal conductivity of nanofluids. Experimental data show that thermal conductivity increases with concentration. Thermal conductivity can also be improved by changing the shape and size of particles, although concentration has the greatest effect on this property. Kiani et al [30] tested different oxide nanofluids with three types of nanoparticles, aluminium oxide (Al_2O_3), copper oxide (CuO), and silver oxide (AgO). Test result showed a significant improvement in the cooling efficiency of the nanofluidic system, of which AgO was the best candidate. Compared to the thermal management system of the pure water battery, the 2% AgO/water nanofluidic system reduced the peak temperature of the battery by about 4.1 K. As shown in Figure 8(a), the addition of nanoparticles significantly improves the heat transfer rate. Figure 8(b) shows the change in the peak temperature of the battery at different volume fractions of AgO nanoparticles at three different concentrations. To investigate the effects of nanoparticle volume fraction and nanofluid flow rates on cooling performance, Bin-Abdun et al. [31] studied the thermophysical properties and heat transfer rates of CuO/deionized water nanofluids with and without sodium dodecyl sulphate (SDS) surfactant. They analysed the effect of flow rate and surfactants on the heat transfer rate of nanofluids with different volume concentrations of 0.08%, 0.16%, and 0.40%. The size and morphology of copper oxide nanoparticles are shown in Figure 8(c). The results showed that the highest heat transfer rate was achieved with CuO/deionized water nanofluid with volume concentration 0.40% and SDS surfactant. The heat transfer rate results with deionized water and copper oxide nanoparticle volume concentrations of 0.08%, 0.16%, and 0.40% at different flow rates are shown in Figure 8(d).

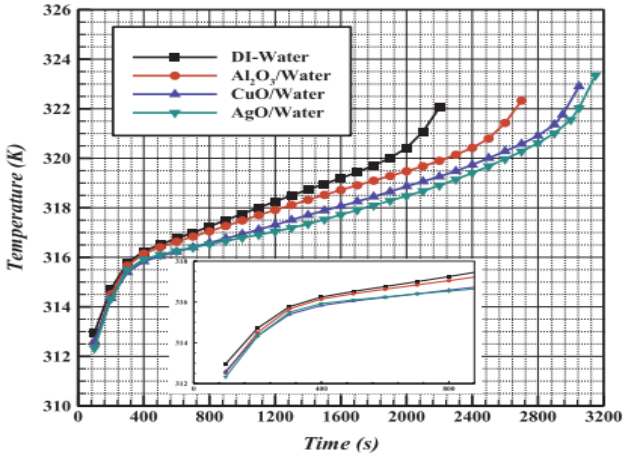

(a)

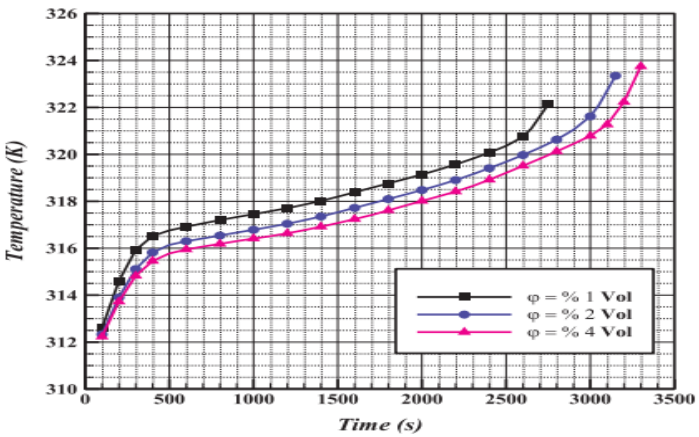

(b)

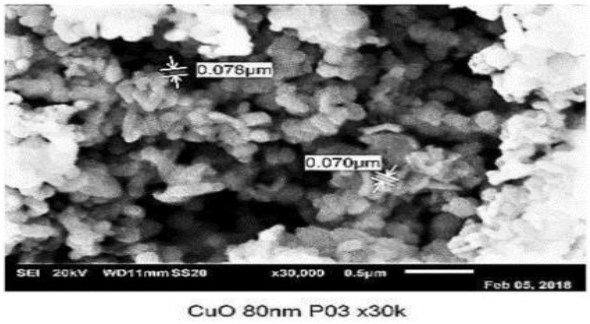

(c)

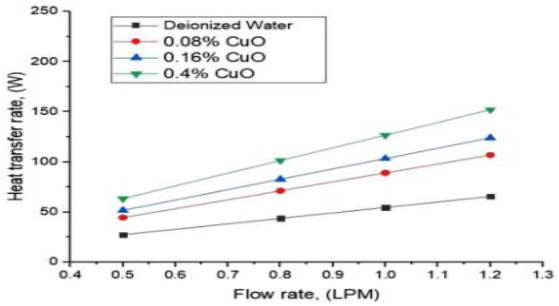

(d)

Figure 8. (a) Effect of various nanofluids on the cooling system [30]. (b) Effect of nanoparticle volume fraction on the cooling performance [30]. (c) SEM images of CuO nanoparticles [31]. (d) Heat transfer rate versus flow rate for deionized water and nanofluids [31].

3.6.2.2. Flow Channel Design Optimization

For indirect cooling methods, the thermal resistance must be considered more accurately due to the addition of channel materials and electrical insulating coatings. To improve the cooling capacity of the cooling system, the system structure can be optimized. In case of indirect liquid cooling, the coolant must pass through certain channels. However, different channel designs can have different effects on BTMS thermal efficiency and power consumption, which is why researchers have conducted many studies on channels.

Ye et al. [32] designed a multichannel parallel cold plate (Figure 9a). In his study a complex heat transfer model was created for the entire module, which included batteries, two cooling plates, silicone gel pads and coolant. An orthogonal experimental design with numerical analysis was applied to optimize the main parameters of the module. The geometry of the plate was further optimized using the surrogate model method. The plate with optimized geometry was reconstructed into the thermal model of the module for analysis. The comparison showed that the maximum and minimum temperature difference of the heat was reduced by 5.24% and the pressure drop was reduced by 16.88%. Analysis of the orthogonal design concluded that the battery temperature difference and pressure drop decreased as the coolant channel cross-section and number increased when coolant flow was constant at the inlet. Quian et al. [33] designed a parallel cold plate with multiple channels. The effects of channel number, flow direction, mass flow, and channel width on battery temperature were investigated using numerical simulation. It is found that the mini-channel cold plate thermal management system provides good cooling performance in controlling the temperature of the battery. Only the 2-channel cold plate can keep the maximum temperature below 40°C for more than half discharge times. The more channels, the better the cooling capacity of the BTMS. Even so, there are no obvious advantages to a cold plate with more than five channels. The maximum temperature and temperature difference can be reduced by increasing the inlet mass flow which is more effective than other methods. However, this costs energy consumption. Increasing the channel width can reduce power consumption. When channel width was changed from 3 mm to 6 mm, the pressure drop is reduced by 55%. Due to the higher heat production of the near electrode area and the different cooling effect of each battery, it is very difficult to reduce the temperature difference below 5°C. Huo et al. [34] designed a parallel cold plate with multiple channels. The effects of channel number, flow direction, mass flow, and ambient temperature on battery temperature were investigated using numerical simulation.

Huang et al. [35] used streamlined channels for indirect liquid cooling, as shown in Figure 9b. They found that this channel can effectively reduce the fluid flow resistance and improve the temperature distribution of the battery. Straight channel and streamlined channel were investigated by numerical solution. It has been observed that for typical straight channel designs, even-channel plates always have a higher resistance to flow than odd-numbered plates. At a mass flow rate of 0.005 kg/s, the pressure drop can be as high as 6581 Pa and 6043 Pa for four and six typical straight channel numbers. When using streamlined channels, the maximum pressure drop is only 3877 Pa. Thus, streamlined channels can effectively reduce pressure loss and avoid direct flow effect, especially in paired channel cooling plates. The temperature difference between streamlined designs with different number of channels is quite similar to a typical straight 5-channel design, which means that the streamlined duct design can maintain the cooling capacity at the same level as a normal straight duct design. The effect of different numbers of channels on the cooling capacity can be controlled by adopting the concept of the streamlined shape of the mini-channel cooling plate. Shetty et al. [36] analysed the performance of streamline cooling plate

with different configurations in a 3, 4, 5, 6, and 7 channel. The purpose of the analysis is to determine the optimal configuration of the cold plate. In addition, the performance of the optimal plate configuration is evaluated at different temperatures between 300 and 328 K. The results show that the streamline plate perform is satisfactorily at different temperatures and the 7-channel configuration performs best at 328 K. The maximum temperature of the solid plate is 302.677 K with a mass flow rate of 0.005 kg/s, which is well within the optimal operating temperature range for a Li-ion battery.

Wei et al. [37] used a U-shaped serpentine channel cold plate (Figure 9c) to reduce the resistance of liquid flow in the channel. His work presented a method based on response surface methodology (RSM) and non-dominated sorting genetic algorithm II (NSGA-II) to achieve optimization of operating parameters with relatively low current resistance. These methods can be used to quickly obtain optimized operating parameters to balance the maximum temperature, average temperature and cold plate pressure drop in BTMS. The results can guide the design of a battery thermal management operational strategy. When the flow rate changes from 0.0019 to 0.0249 kg/s, the pressure drop increases from 27.77 Pa to 1360.47 Pa. The average temperature increases to 9.93°C when the inlet temperature increases from 20 to 30°C. Although increasing the flow rate and lowering the inlet temperature can improve the cooling efficiency of the liquid cold plate, a flow rate greater than 0.0249 kg/s does not significantly affect the temperature uniformity of the liquid cold plate. Optimizing BTMS operating parameters is critical to achieving better overall liquid cold plate performance. Based on the RSM design, regression models are obtained for average temperature, maximum temperature difference and pressure drop with coefficients of variation (C.V) below 0.3%, which ensures the accuracy of the regression models. The average temperature and pressure drop deviations between model predictions and CFD simulations are less than 11%. Fan et al. [38] has designed a U-shape serpentine channel with elliptical grooves (Figure 9d) and secondary channels. The effects of width of the main channel and number of elliptical grooves were investigated using numerical solution. When the width of the main channel (D) increases from 4mm to 10mm, the maximum temperature (Tmax) and average temperature (ΔTavg) decrease by 2.67℃ and 1.32K respectively. When D is 10mm, Tmax and ΔTavg are 39.33°C and 2.74K respectively. Only the design with D of 10mm reached the temperature target of the battery module with Tmax below 40°C and ΔTavg below 3°C. This shows that a liquid cooling plate with a wider D is useful for cooling the battery module, and the larger the D, the more coolant can access the liquid cooling plate, which is more useful for heat transfer. As the number of elliptical grooves increases from 4 to 7, the Tmax and ΔTavg of the battery module increase by 0.84°C and 0.49615K, respectively. This shows that changing the number of elliptical grooves has little effect on the temperature of the battery module. Jayarajan et al. [39] used a u-shaped serpentine channel cold plate with zig-zag pattern (Figure 9e). The effects of number of the cooling channel, change in channel width, inlet mass flow rate, change in heat flux and change in inlet coolant temperature were investigated using numerical solution. Results showed that the cold plate with a larger number of channels had good temperature uniformity (Tσ), that is, Tσ = 3.2 K for the 13-channel cold plate and Tσ = 6.01 K for the 3-channel cold plate, and the maximum temperature Tmax for the 3-channel cold plate was 330.84 K, while for the 13-channel cold plate it was 316 K. This trend was reversed for pressure drop. As the number of channels increased from 3 to 13, the resistance increased. Therefore, the 13-channel cold plate showed a higher pressure drop (13.34 × 103 Pa) compared to the 3-channel cold plate (3.84 × 103 Pa). The heat transfer rate followed the same trend as Tmax and Tσ, that is due to the removal of material, which resulted in a decrease in the conductivity of the cold plate. As the number of channels increased, the heat transfer rate decreased. The pressure drop was too high in channels 11 and 13, and the 3-channel cold plate had poor temperature uniformity. Increasing the channel width significantly reduced the pressure and did not show significant changes in other parameters. 5-channel width 16 mm and 18 mm and 7-channel width 16 mm showed an improvement in pressure drop. The increase in mass flow reduced the maximum temperature and improved the standard surface temperature and heat transfer rate, but increases the pressure drop by almost 49%. Inlet cooling temperature drop showed an improvement in maximum temperature drop for the 5 and 7-channel models at discharge rates of 2C, 3C and 4C.

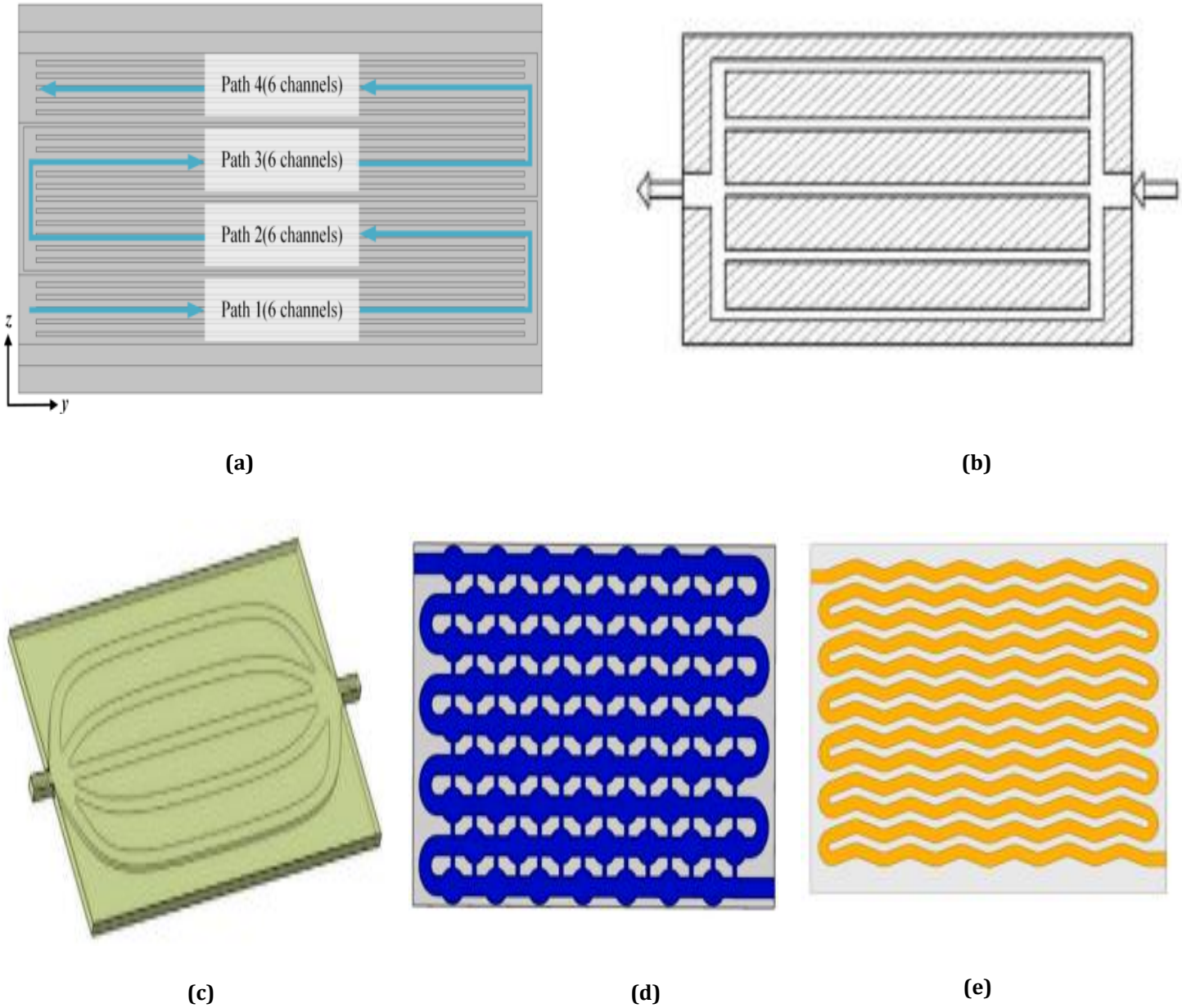

Figure 9. Typical design of the channel: (a) Parallel channel [32]. (b) Streamlined channel [35].(c) U-shaped serpentine channel [37]. (d) U-shaped serpentine channel with elliptical grooves [38]. (e) U-shaped serpentine channel with zig-zag pattern [39].

Wang et al. [40] proposed a new type of spider web channel cold plate (Figure 10a) and investigated its cooling effect and thermal balance performance for a pouch lithium-ion battery. The battery heat generation model was obtained by numerical simulation, which accurately simulates the temperature distribution of the battery with a discharge rate of 12 C. A three-factor, four-level orthogonal test set was used to find the best combination of different structural parameters of the spider web channel. The simulation results showed that the cold plate performance was most affected by channel width (l), second by number of channels (n), and least affected by channel angle (α). The best combination obtained from the orthogonal experiment contained l4 = 3 mm, n4 = 11 and α3 = 120° where the Li-ion battery had the lowest temperature (37.892°C) and the smallest temperature difference (8.864 °C). The pump loss was lower on the cold plate (27.06 Pa). Li et al. [41] analysed the performance of four different cold plates namely U-shaped, aerofoil, honeycomb and convex structure (Figure 10b). After comparing and analysing the four liquid-cooled plates, it was found that the convex-shaped cooling plate had the lowest pressure loss at different flow rates, and the resistances of the honeycomb structure

and the air foil structure were the highest. The heat exchange characteristics of several cooling plates were basically the same, but the temperature uniformity of the cell structure was the worst, and the cooling performance of the cooling plate was greatly affected by the flow rate. The maximum temperature of this type of plate always exists at a certain mass flow, which is difficult to remove. To ensure a temperature difference (≤10 K) between the inlet and outlet of the cooling plate, it is necessary that the mass flow of the cooling plate is at least 0.0223 kg/s. Increasing the mass flow is an effective way to cool the battery in a short period of time. Luo et al. [42] has developed a new cold plate called constructal cold plate (Figure 10c) using the constructal theory. The constructal pate was analysed and its results were compared with conventional straight and serpentine plate. Compared to the conventional cold plate, the constructal cold plate has better performance. Compared with a straight channel cold plate, the constructal cold plate allows the cell to reach its optimal operating temperature earlier, reducing TimeT (time required for battery average temperature to drop to 25 ◦C) and TimeΔT (time required for battery maximum temperature differential to drop to 5 ◦C) by 15.25% and 10.58%, respectively, and Δp (pressure drop) by 22.89%. Compared with the serpentine cold plate, the constructal cold plate has a slightly worse cooling effect, but the flow resistance is greatly reduced, and the pressure drop of the serpentine cold plate is about ten times greater than that of the structural cold plate.

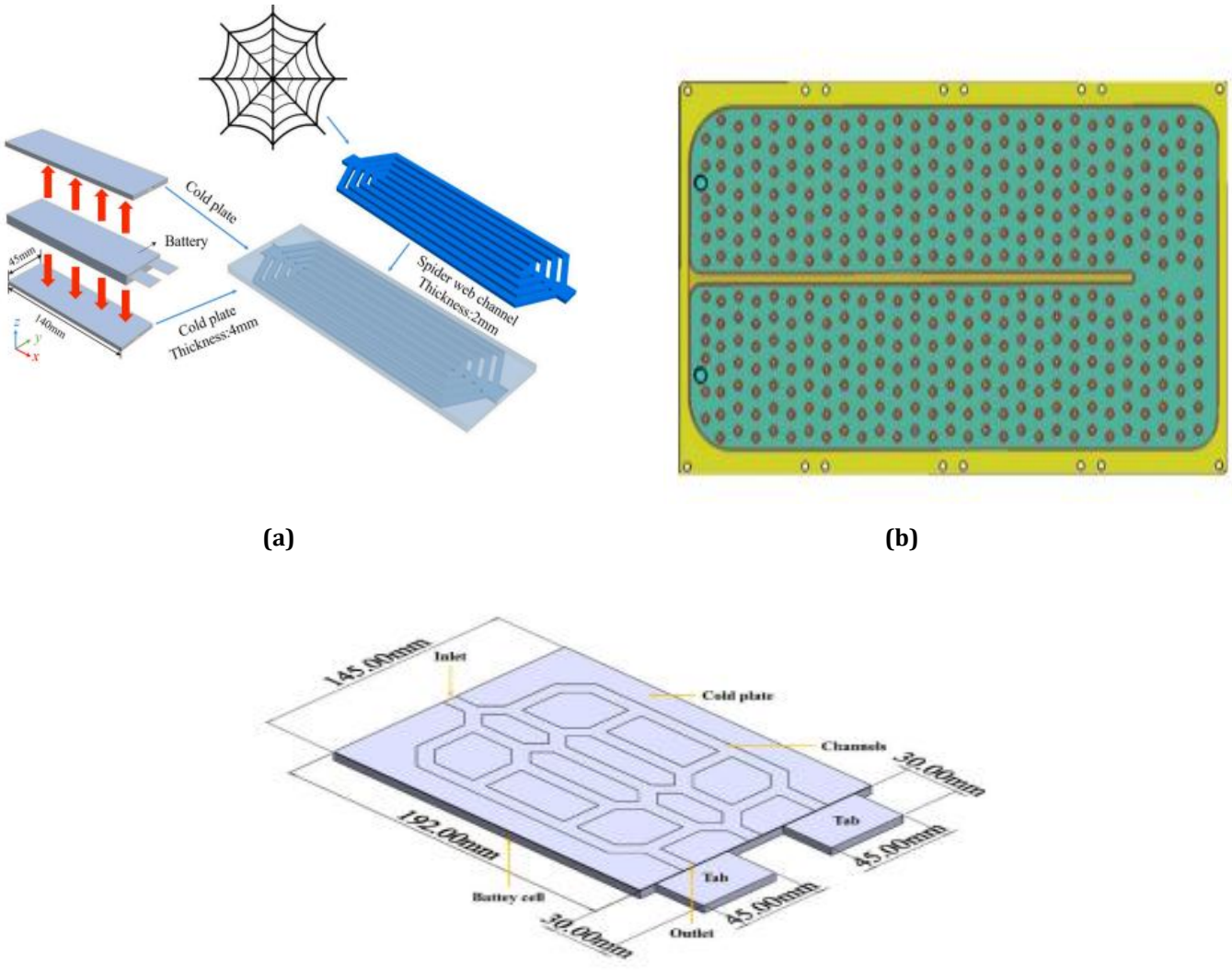

Figure 10. (a) Spider web channel [40]. (b) cooling plate with convex structure [41]. (c) Schematic design of constructal cold plate [42].

Based on the typical channel structure, parallel channels and serpentine channels are gradually replaced by channels with better cooling effect. Monica et al. [43] illustrates six cold plate designs (Figure 11a) that were compared with the same channel volume, including straight, serpentine, U-shaped, pumpkin- shape, spiral, and hexagonal structure. Numerical analysis found that despite the large pressure drop, the snake channel and hexagonal channel have good cooling properties and can significantly improve the temperature distribution of the battery. In addition, Chen et al. [44] investigated the cooling of BTMS based on a parallel mini-channel cold plate (PMCP) and designed three different PMCP flow channels (type I, Z and U). PMCP cooling efficiency was found to be significantly improved by changing the edge width and channel width of the cold plate. Chen's study also constructed three symmetrical PMCPS, as shown in Figure 11b. The results showed that the symmetrical cold plate can control the maximum temperature and temperature difference of the battery module in a low range, and it helps to reduce the energy consumption of the system.

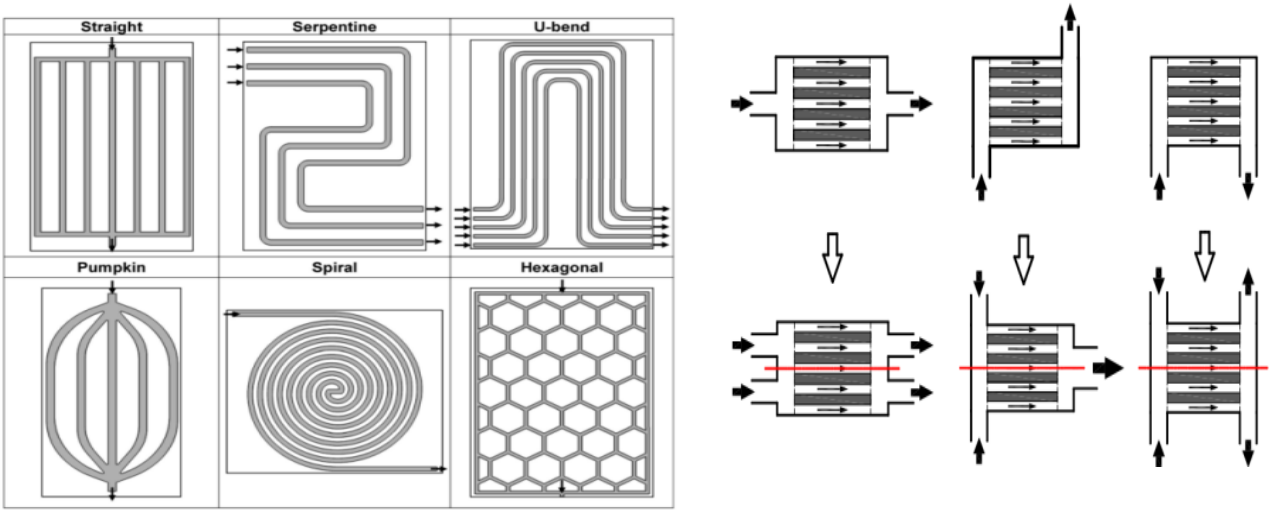

(a) **(b)**

Figure 11. (a) Design of six cold plate channels [43]. (b) Three symmetric PMCPs [44].

By optimizing the flow channel geometry, topology optimization (TO) can be used to increase the heat transfer efficiency of the cold plate and decrease flows losses. A new channel structure cooling plate for TO was designed by Chen et al. [45] as illustrated in Figure 12. From numerical analysis it was revealed that in comparison with the traditional rectangular channel cold plate (RCP) and serpentine channel cold plate (SCP), the topology optimization cold plate (TCP) has a higher heat transfer coefficient. At the same inlet pressure, TCP-RCP has a maximum temperature, temperature difference and temperature standard deviation of 0.27%, 19.5% and 24.66% lower than that of the rectangular channel cold plate (RCP).

Thus, the cooling performance of indirect liquid cooling can be improved by adjusting the channel structure and configuration, including channel geometry, channel width, channel spacing, number of inlets and outlets, microchannels, etc.

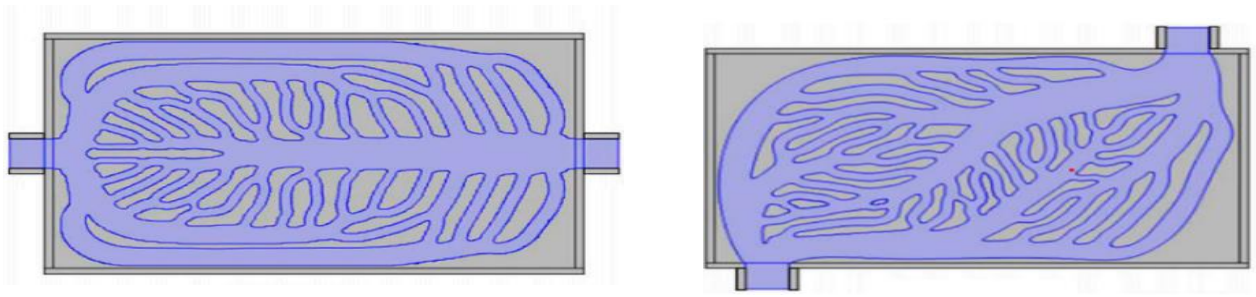

(a) TCP-RCP **(b) TCP-SCP**

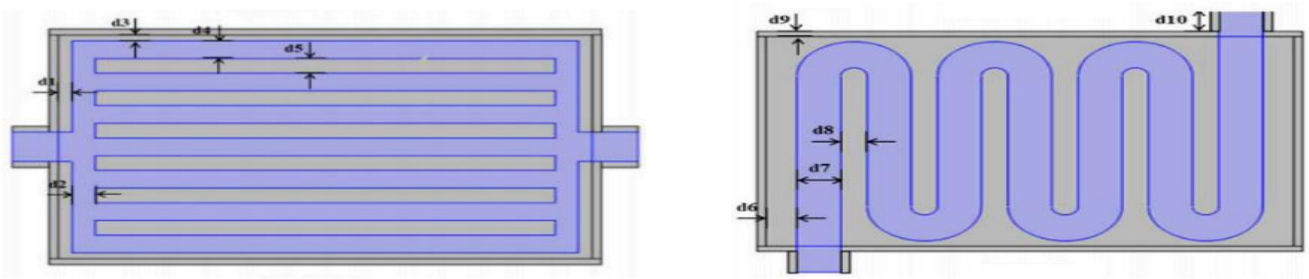

(c) RCP **(d) SCP**

Figure 12. Cold plate diagram [45].

3.6.2.3. Structure optimization of liquid cooling system

The number of cooling channel and flow rate of coolant have an important influence on the performance of the liquid cooled BTMS. Along with this the position of the cold plates, number of cold plates and the contact area between the cold plate and battery is also influences the cooling performance.

Using a multichannel flat tube (MCFT), Ren et al. [46] developed a method for bottom liquid cooling (BLC) to analyse the temperature distribution of the battery module according to the BLC method, a comparative test with passive cooling was performed. Figure 13a shows the outline of a module consisting of LIB, MCFT, and aluminium shell. The results indicated that the BLC, which was based on an MCFT, significantly enhanced the temperature uniformity of the module and also minimized the overall temperature increase of its battery module. Darcovich et al. [47] investigated the performance of the cooling system by placing cold plates on the bottom and side of the battery. The results showed that the side plate can keep the temperature on the cell surface quite constant between 304.2 and 304.6 K, while the temperature range of cooling with the cold plate can be seen as almost 5 K under the same test conditions. It is understood that chemical and electrochemical systems work well at this temp. Since side cooling has more contact areas with the battery than bottom cooling, its maximum temperature is lower and temperature uniformity is better. Qian et al. [33] utilized two distinct cooling systems that were constructed using different numbers of cold plates (Figure 13b). The results of simulation showed that three cold plates helped to improve the temperature distribution. When the coolant flow rate is 1 × 10-3 kg/s, the difference between the maximum battery temperature and the temperature decreases by 13.3% and 43.3%. Deng et al. [48], designed six different cold plate layout patterns (Figure 13c) to investigate the effect of battery heat dissipation. The maximum temperature of the battery decreased as the number of cold plates increased. When the number of cold plates increased to five, the heat removal performance of the system was the best. The author emphasized that if there are the same number of cold plates, equally placing the cold plates near the buffer battery is useful to lower the maximum temperature. Therefore, the side cold plates should be selected as much as possible within the allowable cost and power range, and the number of cold plates should be increased. Jin et al. [49] investigated the effect of battery layout structure on the performance of thermal runaway in cell-to-chassis (CTC) systems. The findings indicated that the battery system's safety can be enhanced by modifying the batteries' structure. By changing the arrangement of the battery from a conventional in-line configuration to a brick configuration, the propagation of thermal runoff in the battery can be effectively prevented due to the lower thermal peak current and heat in the brick configuration is transferred to more adjacent batteries.

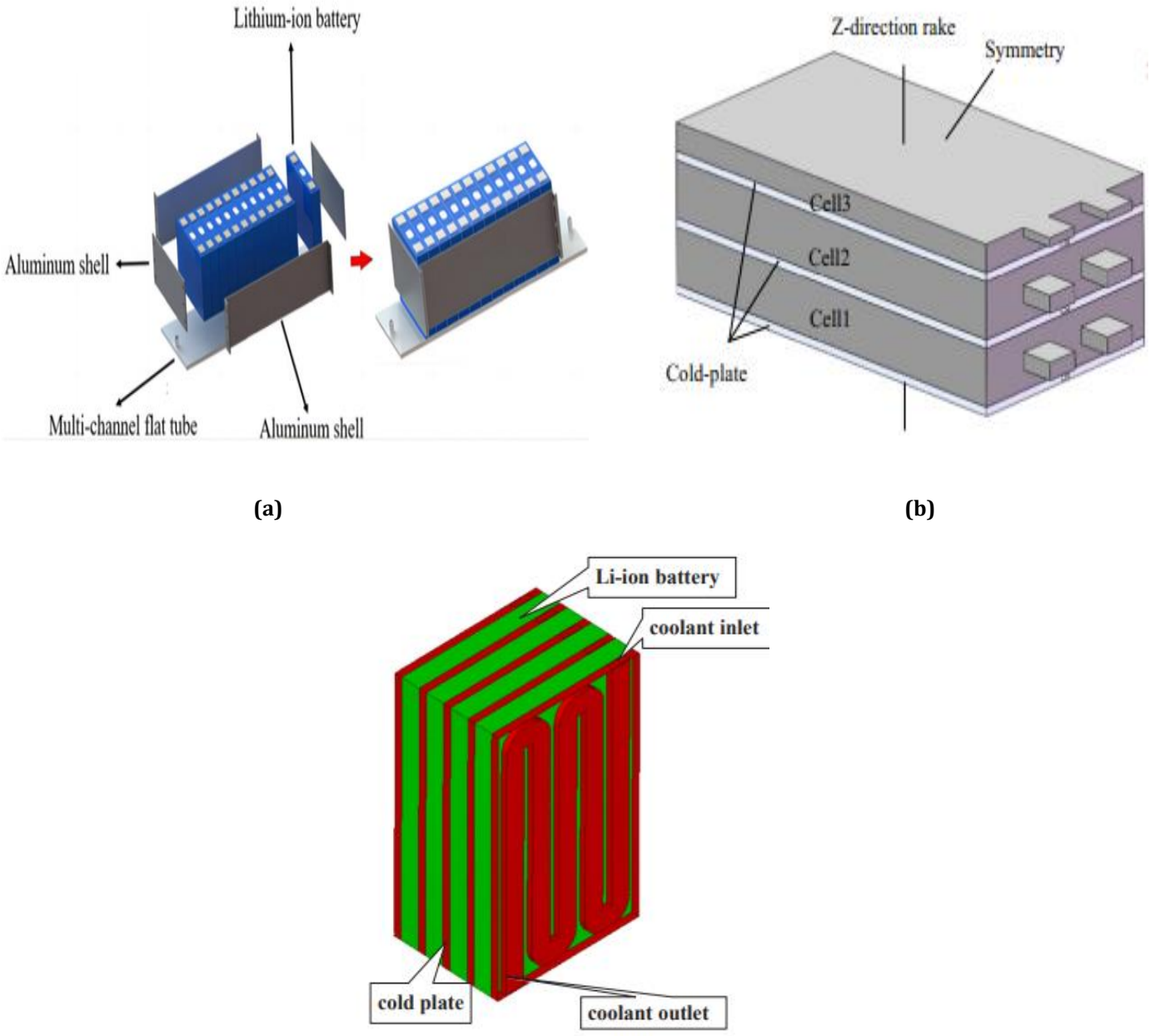

(a) **(b)**

(c)

Figure 13. Cold plate diagram (a) structure diagram of the BLC based on MCFT [46]. (b) bottom liquid cooling [48]. (c) side liquid cooling [49].

Fu et al. [50] analysed the heat dissipation capacity of a liquid cold plate battery with different heat transfer fins (Figure 14a). Compared with the liquid cold plate without fins, the liquid cold plate with 8 mm - 15° fins lowers the maximum temperature of the battery by 1.75 K when the temperature difference is 0.32 K. When the angle of the fins changes from 30° to 45°, the peak temperature and the battery temperatures the difference decreases as the rib length increases. Thus, adding heat transfer fins inside the liquid cold plate can significantly reduce the peak temperature of the battery module and the temperature difference between the cells. Om et al. [51] designed a liquid cooled plate (LCP) with three different angle fin arrangements inline (Figure 14b), incline (Figure 14c) and louvered (Figure 14d). The flow and heat transfer properties of these fins are compared through experimental and numerical simulation studies. From the results, it is observed that louvered fin arrangement has the highest value of Nusselt number followed by inline and inclined

arrangement. The designed LCP with a different arrangement of fins can keep the surface temperature of the heater block below 50 °C at Reynolds number 400-1200.

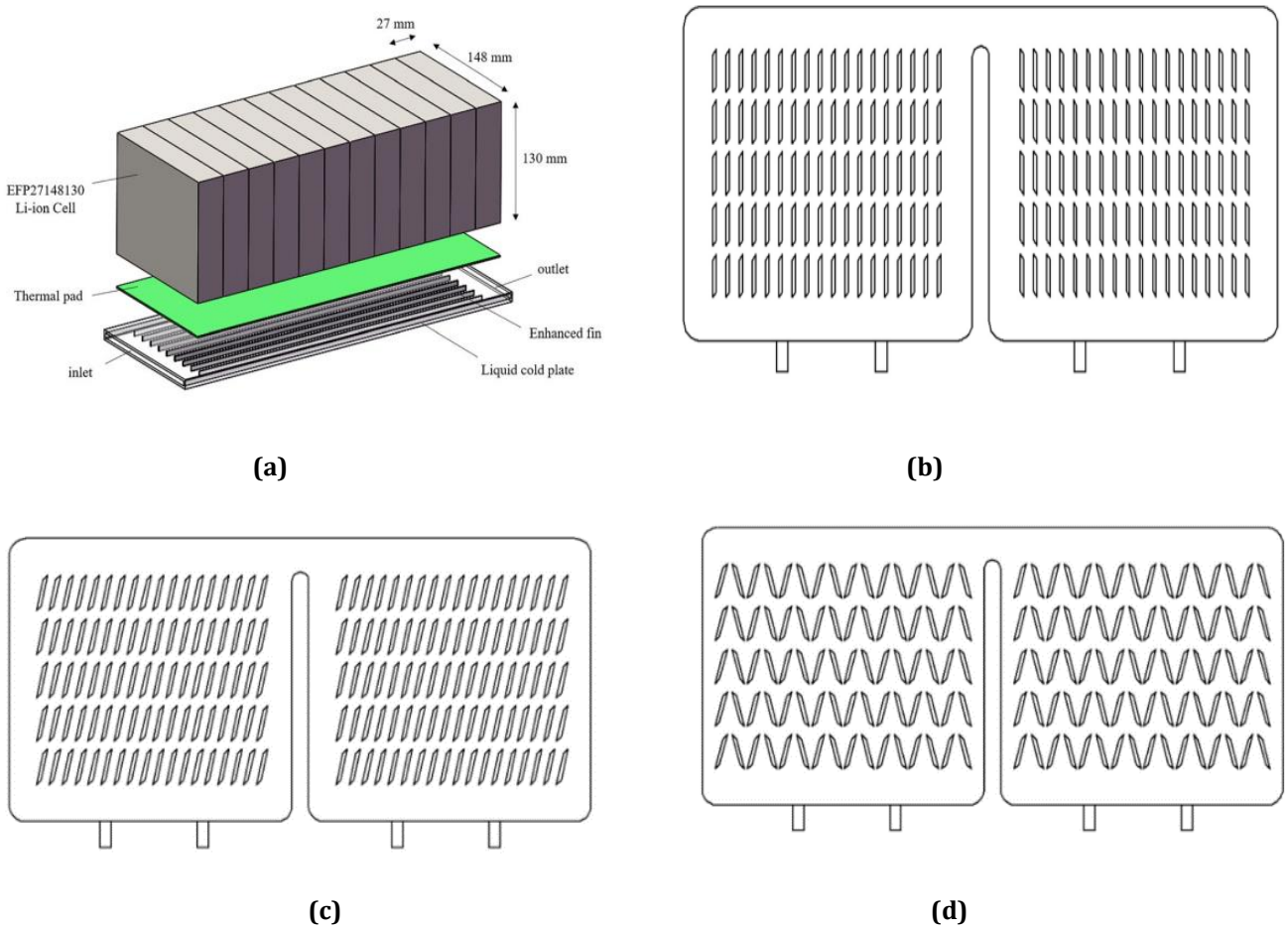

Figure 14. (a) Module components [51]. (b) Inline oblique fin arrangement [52]. (c) Incline oblique fin arrangement [52]. (d) Louvered oblique fin arrangement [52].

Summary and prospect

Based on the above studies, liquid cooling is a very effective thermal management technique that can control the battery temperature and temperature difference within an acceptable range. This paper reviews the literature on indirect liquid cooling of BTMS. The review provides a comprehensive overview of design improvement techniques and highlights their effectiveness in improving cooling performance. Factors such as selection of coolant, flow rate of coolant, temperature and geometry and structure of system greatly affect overall system performance. Future research should focus on developing improved liquid coolants, simplifying cooling channels and optimizing heat transfer of the cooling plates. The research of different cooling methods with different compatibility holds the potential for liquid cooling solutions for commercial electric vehicles. In summary, this study highlights the huge potential of liquid-cooled BTMS to improve thermal management of Li-ion batteries, which requires further development and optimization of liquid cooling technology.

Nomenclature

LIB	Lithium-ion Battery
BTMS	Battery Thermal management system
PCM	Phase change material
SOC	State of charge
SOH	State of health
SEI	Solid electrolyte interface
DRS	Direct refrigerant system
CFD	Computational fluid dynamics
GPM	Grams per minute
Al_2O_3	Aluminium oxide
TiO_2	Titanium dioxide
CuO	Copper oxide
AgO	Silver oxide
SDS	Sodium dodecyl sulphate
RSM	Response surface methodology
NSGA-II	Non-dominated sorting genetic algorithm II
C.V	Coefficients of variation
D	Width of the main channel (mm)
Tmax	Maximum temperature (°C)
ΔTavg	Average temperature (°C)
Δp	Pressure drop (pa)
Tσ	Temperature uniformity
PMCP	Parallel mini-channel cold plate
TO	Topology optimization
MCFT	Multichannel flat tube
BLC	Bottom liquid cooling
CTC	Cell-to-chassis

REFERENCES

[1] Zhao, C.; Zhang, B.; Zheng, Y.; Huang, S.; Yan, T.; Liu, X. Hybrid Battery Thermal Management System in Electrical Vehicles: A Review. *Energies 2020, 13, 6257.* 6257; Doi: https://doi.org/10.3390/en13236257

[2] Aneke, M.; Wang, M. Energy storage technologies and real life applications-A state of the art review. *Appl. Energy 2016, 179, 350–377*; Doi: http://dx.doi.org/10.1016/j.apenergy.2016.06.097

[3] Liu, J.; Chen, H.; Huang, S.; Jiao, Y.; Chen, M. Recent Progress and Prospects in Liquid Cooling Thermal Management System for Lithium-Ion Batteries. *Batteries 2023, 9, 400*; Doi: https://doi.org/10.3390/batteries9080400

[4] Wang, Q.; Jiang, B.; Li, B.; Yan, Y. A critical review of thermal management models and solutions of lithium-ion batteries for the development of pure electric vehicles. Renew. Sustain. *Energy Rev. 2016, 64, 106–128*; Doi: http://dx.doi.org/10.1016/j.rser.2016.05.033

[5] Kim, J.; Oh, J.; Lee, H. Review on battery thermal management system for electric vehicles. *Appl. Therm. Eng. 2019, 149, 192–212*; Doi: https://doi.org/10.1016/j.applthermaleng.2018.12.020

[6]Sourav Singh Katoch and M Eswaramoorthy 2020 *IOP Conf. Ser.: Mater. Sci. Eng. 912 042005*; Doi: https://doi.org/10.1088/1757-899X/912/4/042005

[7] Wang, Q.; Mao, B.; Stoliarov, S.I.; Sun, J. A review of lithium ion battery failure mechanisms and fire prevention strategies. *Prog. Energy Combust. Sci. 2019, 73, 95*–131; Doi: https://doi.org/10.1016/j.pecs.2019.03.002

[8]Li, B.; Xia, D. Anionic Redox in Rechargeable Lithium Batteries. *Adv. Mater. 2017, 29, 1701054*; DOI: https://doi.org/10.1002/adma.201701054

[9] Lai, Y.; Du, S.; Ai, L.; Ai, L.; Cheng, Y.; Tang, Y.; Jia, M. Insight into heat generation of lithium-ion batteries based on the electrochemical-thermal model at high discharge rates. *Int. J. Hydrog. Energy 2015, 40, 13039–13049*; Doi: https://doi.org/10.016/j.ijhydene.2015.07.079

[10] Bernardi, D.; Pawlikowski, E.; Newman, J. A General Energy Balance for Battery Systems. *J. Electrochem. Soc. 2019, 132, 5–12*; Doi: https://doi.org/10.1149/1.2113792

[11] Fathabadi, H. A novel design including cooling media for Lithium-ion batteries pack used in hybrid and electric vehicles. *J. Power Sources 2014, 245, 495–500*; Doi: https://doi.org/10.1016/j.jpowsour.2013.06.160

[12] Smart, M.C.; Ratnakumar, B.V.; Whitcanack, L.D.; Chin, K.B.; Surampudi, S.; Croft, H.; Tice, D.; Staniewicz, R. Improved Low-Temperature Performance of Lithium-Ion Cells with Quaternary Carbonate-Based Electrolytes. *J. Power Sources 2003, 119-121, 349*-358; Doi: https://doi.org/10.1016/S0378-7753(03)00154-X

[13] Liu, H.; Wei, Z.; He, W.; Zhao, J. Thermal issues about Li-ion batteries and recent progress in battery thermal management systems: A review. *Energy Convers. Manag. 2017, 150, 304–330*; Doi: https://doi.org/10.1016/j.enconman.2017.08.016

[14] Zhao, R.; Gu, J.; Liu, J. An experimental study of heat pipe thermal management system with wet cooling method for lithium-ion batteries. *J. Power Sources 2015, 273, 1089–1097*; Doi: https://doi.org/10.1016/j.jpowsour.2014.10.007

[15] Ramadass PH BW RP, B.; Haran, B.; White, R.; Popov, B.N. Capacity fade of Sony 18650 cells cycled at elevated temperatures Part I. Cycling performance. *J. Power Sources 2002, 112, 606–613*; Doi: https://doi.org/10.1016/S0378-7753(02)00474-3

[16] Chen, K.; Li, Z.; Wang, S. Design of Parallel Air-Cooled Battery Thermal Management System through Numerical Study. *Energies 2017, 10, 1677*; Doi: *https://doi.org/*10.3390/en10101677

[17] Chung, Y.; Kim, M.S. Thermal analysis and pack level design of battery thermal management system with liquid cooling for electric vehicles. *Energy Conversion and Management 196 (2019) 105-116*; Doi: https://doi.org/10.1016/j.enconman.2019.05.083

[18] Tran, TH.; Harmand, S.; Desmet, B.; Filangi, S. Experimental investigation on the feasibility of heat pipe cooling for HEV/EV lithium-ion battery. *Applied Thermal Engineering 63 (2014) 551*-558; Doi: http://dx.doi.org/10.1016/j.applthermaleng.2013.11.048

[19] E, J.; Xu, S.; Deng, Y.; Zhu, H.; Zuo, W.; Wang, H.; Chen, J.; Peng, Q.; Zhang, Z. Investigation on thermal performance and pressure loss of the fluid cold-plate used in thermal management system of the battery pack. *Appl. Therm. Eng. 2018, 145, 552–568*; Doi: https://doi.org/10.1016/j.applthermaleng.2018.09.048

[20] Thakur, A.K.; Prabakaran, R.; Elkadeem, M.R.; Sharshir, S.W.; Arıc, M.; Wang, C.; Zhao, W.; Hwang, J.-Y.; Saidur, R. A state of art review and future viewpoint on advance cooling techniques for Lithium–ion battery system of electric vehicles. *J. Energy Storage 2020, 32, 101771*; Doi: https://doi.org/10.1016/j.est.2020.101771

[21] Ke, Q.; Li, X.; Guo, J.; Cao, W.; Wang, Y.; Jiang, F. The retarding effect of liquid-cooling thermal management on thermal runaway propagation in lithium-ion batteries. *J. Energy Storage 2022, 48, 104063*; Doi: https://doi.org/10.1016/j.est.2022.104063

[22] Jarrett, A.; Kim, I.Y. Design optimization of electric vehicle battery cooling plates for thermal performance. *J. Power Sources 2011, 196, 10359–10368*; Doi: https://doi.org/10.1016/j.jpowsour.2011.06.090

[23] Wang, T.; Zhang, X.; Zeng, Q.; Gao, K. Thermal management performance of cavity cold plates for pouch Li-ion batteries using in electric vehicles. *Energy Sci Eng. 2020; 8:4082–409;*. Doi: https://doi.org/10.1002/ese3.798

[24] Aldosry, A.M.; Zulkifli, R.; Wan Ghopa, W.A. Heat Transfer Enhancement of Liquid Cooled Copper Plate with Oblique Fins for Electric Vehicles Battery Thermal Management. *World Electr. Veh. J. 2021, 12, 55*; Doi: https://doi.org/10.3390/wevj12020055

[25] Pan, C.; Tang, Q.; He, Z.; Wang, L.; Chen, L. Structure Optimization of Battery Module With a Parallel Multi-Channel Liquid Cooling Plate Based on Orthogonal Test. J. Electrochem. *Energy Convers. Storage 2020, 17, 021104*; Doi: https://doi.org/10.1115/1.4045197

[26] Panchal, S.; Khasow, R.; Dincer, I.; Agelin-Chaab, M.; Fraser, R.; Fowler, M. Thermal design and simulation of mini-channel cold plate for water cooled large sized prismatic lithium-ion battery. *Appl. Therm. Eng. 2017, 122, 80*–90; Doi: https://doi.org/10.1016/j.applthermaleng.2017.05.010

[27] Malik, M.; Dincer, I.; Rosen, M.A.; Mathew, M.; Fowler, M. Thermal and electrical performance evaluations of series connected Li-ion batteries in a pack with liquid cooling. *Appl. Therm. Eng. 2018, 129, 472–481*; Doi: https://doi.org/10.1016/j.applthermaleng.2017.10.029

[28] Zakaria, I.; Azmi, W.H.; Mohamed, W.A.N.W.; Mamat, R.; Najafi, G. Experimental Investigation of Thermal Conductivity and Electrical Conductivity of Al2O3 Nanofluid in Water—Ethylene Glycol Mixture for Proton Exchange Membrane Fuel Cell Application. *Int. Commun. Heat Mass Transf. 2015, 61, 61–68*; Doi: https://doi.org/10.1016/j.applthermaleng.2017.10.029

[29] Maheshwary, P.B.; Handa, C.C.; Nemade, K.R. A comprehensive study of effect of concentration, particle size and particle shape on thermal conductivity of titania/water based nanofluid. *Appl. Therm. Eng. 2017, 119, 79–88*; Doi: https://doi.org/10.1016/j.applthermaleng.2017.03.054

[30] Kiani, M.; Omiddezyani, S.; Houshfar, E.; Miremadi, S.M.; Ashjaee, M.; Nejad, A.M. Lithium-ion battery thermal management system with Al2O3/AgO/CuO nanofluids and phase change material. *Appl. Therm. Eng., 2020, 180, 115840*; Doi: *https://doi.org/*10.1016/j.applthermaleng.2020.115840

[31] Bin-Abdun, N.A.; Razlan, Z.M.; Bakar, S.A.; Voon, C.H.; Ibrahim, Z.;Wan, W.K.;Ridzuan , M.J.M. Heat transfer improvement in simulated small battery compartment using metal oxide (CuO)/deionized water nanofluid. *Heat Mass Transfer, 2019, 56, 399–406*; Doi: https://doi.org/10.1007/s00231-019-02719-6

[32] Ye, B.; Haque Rubel, M.R; Li, H. Design and Optimization of Cooling Plate for Battery Module of an Electric Vehicle. *Appl. Sci. 2019, 9, 754*; Doi: https://doi.org/doi:10.3390/app9040754

[33] Qian, Z.; Li, Y.; Rao, Z. Thermal performance of lithium-ion battery thermal management system by using mini-channel cooling. *Energy Conversion and Management 126 (2016) 622–631*; Doi: http://dx.doi.org/10.1016/j.enconman.2016.08.063

[34] Huo, Y.; Rao, Z.; Liu, X.; Zhao, J. Investigation of power battery thermal management by using mini-channel cold plate. *Energy Convers. Manag. 2015, 89, 387–395*; Doi: https://doi.org/10.1016/j.enconman.2014.10.015

[35] Huang, Y.; Mei, P.; Lu, Y.; Huang, R.; Yu, X.; Chen, Z.; Roskilly, A.P. A novel approach for Lithium-ion battery thermal management with streamline shape mini channel cooling plates. *Appl. Therm. Eng. 2019, 157, 113623*; Doi: https://doi.org/10.1016/j.applthermaleng.2019.04.033

[36] Shetty, D.; Vivek, V.; Pradeep, R.; Mohammad, Z.; Irfan, A.B.; Chandrakant, K. Computational flow analysis of different streamline cooling plates for thermal management of lithium-ion battery. *Cogent Engineering (2022), 9: 2048996*; Doi: https://doi.org/10.1080/23311916.2022.2048996

[37] Wei, L.; Zou, Y.; Cao, F.; Ma, Z.; Lu, Z.; Jin, L. An Optimization Study on the Operating Parameters of Liquid Cold Plate for Battery Thermal Management of Electric Vehicles. *Energies 2022, 15, 9180*; Doi: https://doi.org/10.3390/en15239180

[38] Fan, L.; Li, J.; Chen, Y.; Zhou, D.; Jiang, Z.; Sun, J. Study on the cooling performance of a new secondary flow serpentine liquid cooling plate used for lithium battery thermal management. *International Journal of Heat and Mass Transfer 218 (2024) 124711*; Doi: https://doi.org/10.1016/j.ijheatmasstransfer.2023.124711

[39] Jayarajan, S.A.; Azimov, U. CFD Modeling and Thermal Analysis of a Cold Plate Design with a Zig-Zag Serpentine Flow Pattern for Li-Ion Batteries. *Energies 2023, 16, 5243*; Doi: https://doi.org/10.3390/en16145243

[40] Wang, J.; Liu, X.; Liu, F.; Liu, Y.; Wang, F.; Yang, N. Numerical optimization of the cooling effect of the bionic spider-web channel cold plate on a pouch lithium-ion battery. *Case Studies in Thermal Engineering 26 (2021) 101124*; Doi: https://doi.org/10.1016/j.csite.2021.101124

[41] Li, M.; Wang, J.; Guo, Q.; Li, Y.; Xue, Q.; Qin, G. Numerical Analysis of Cooling Plates with Different Structures for Electric Vehicle Battery Thermal Management Systems. *J. Energy Eng., 2020, 146(4): 04020037*; DOI: https://doi.org/10.1061/(ASCE)EY.1943-7897.0000648

[42] Luo, L.; Liao, Z.; Wang, Z.; Liu, Y.; Zhong, J.; Hong, X. Investigation of the heat generation characteristics of lithium-ion battery and orthogonal analysis of its constructal cold plate structure parameters. *Case Studies in Thermal Engineering 52 (2023) 103750*; Doi: https://doi.org/10.1016/j.csite.2023.103750

[43] Monika, K.; Datta, S.P. Comparative assessment among several channel designs with constant volume for cooling of pouch-type battery module. *Energy Convers. Manag. 2022, 251, 114936*; Doi: https://doi.org/10.1016/j.enconman.2021.114936

[44] Chen, K.; Chen, Y.; Song, M.; Wang, S. Multi-parameter structure design of parallel mini-channel cold plate for battery thermal management. *Int. J. Energy Res. 2020, 44, 4321–4334*; Doi: https://doi.org/10.1002/er.5200

[45] Chen, F.; Wang, J.; Yang, X. Topology optimization design and numerical analysis on cold plates for lithium-ion battery thermal management. *Int. J. Heat Mass Transf. 2022, 183, 122087*; Doi: https://doi.org/10.1016/j.ijheatmasstransfer.2021.122087

[46] Ren, R.; Zhao, Y. Experimental study on the bottom liquid cooling thermal management system for lithium-ion battery based on multichannel flat tube. *Appl. Therm. Eng., 2023, 219(C), 119636*; Doi: https://doi.org/10.1016/j.applthermaleng.2022.119636

[47] Darcovich, K.; MacNeil, D.D.; Recoskie, S.; Cadic, Q.; Ilinca, F. Comparison of cooling plate configurations for automotive battery pack thermal management. *Appl. Therm. Eng. 2019, 155, 185*; Doi: https://doi.org/10.1016/j.applthermaleng.2019.03.146

[48] Deng, T.; Zhang, G.; Ran, Y.; Liu, P. Thermal performance of lithium ion battery pack by using cold plate. *Appl. Therm. Eng. 2019, 160,* 114088; Doi: https://doi.org/10.1016/j.applthermaleng.2019.114088

[49] Jin, C.; Sun, Y.; Yao, J.; Feng, X.; Lai, X.; Shen, K.; Wang, H.; Rui, X.; Xu, C.; Zheng, Y.; et al. No thermal runaway propagation optimization design of battery arrangement for cell-to-chassis technology. *eTransportation 2022, 14, 100199*; Doi: https://doi.org/10.1002/er.7990

[50] Fu, J.; Xu, X.; Li, R. Battery module thermal management based on liquid cold plate with heat transfer enhanced fin. *Int J Energy Res. 2019;43:4312–4321*; Doi: https://doi.org/10.1002/er.4556

[51] Om, N.I.; Zulkifli, R.; Gunnasegaran, P. Influence of the oblique fin arrangement on the fluid flow and thermal performance of liquid cold plate. *Case Studies in Thermal Engineering 12 (2018) 717–727*; Doi: https://doi.org/10.1016/j.csite.2018.09.008